catalysts

MDPI

Article

Polymerization of Alkylsilanes on ZIF-8 to Hierarchical Siloxane Microspheres and Microflowers

Lin Yang, Congjia Xie, Yizhou Li, Lei Guo, Minfang Nie, Jinping Zhang, Zhiying Yan, Jiaqiang Wang * and Wei Wang *

Yunnan Provincial Collaborative Innovation Center of Green Chemistry for Lignite Energy, Yunnan Province Engineering Research Center of Photocatalytic Treatment of Industrial Wastewater, The Universities' Center for Photocatalytic Treatment of Pollutants in Yunnan Province, School of Energy, School of Chemical Sciences & Technology, Yunnan University, Kunming 650091, China; 15687376526@163.com (L.Y.); 18288251980@163.com (C.X.); zh111111ou@sina.com (Y.L.); guolei28@yeah.net (L.G.); 18487159609@163.com (M.N.); 18810264274@163.com (J.Z.); zhyyan@ynu.edu.cn (Z.Y.)

* Correspondence: jqwang@ynu.edu.cn (J.W.); wangwei2@ynu.edu.cn (W.W.); Tel.: +86-871-6503-1567 (J.W.); +86-871-6461-9626 (W.W.)

Academic Editor: Carl Redshaw
Received: 6 December 2016; Accepted: 1 March 2017; Published: 3 March 2017

Abstract: The use of metal-organic frameworks (MOFs) in the polymerization field remains comparatively rare up to now, let alone studies on the fabrication of polymer microstructures through a MOFs-catalyzed assembly process. Zeolitic imidazolate framework-8 (ZIF-8), a well-known MOF for its chemical and thermal stabilities, was used to induce a polymerization reaction of saturated alkylsilanes for the first time. The reaction temperature was found to be critical for morphology control of the polymerized ZIF-siloxane composites. The polymerization of alkylsilanes by ZIF-8 at room temperature resulted in siloxane microspheres while rose petal-like microstructures were obtained at higher temperature. The effects of the reaction time on the structures of the polymerization products were also investigated and the polymerization reaction process was proposed. This work expands the field of MOFs' applications and develops a reasonable method for the multidimensional assembly of MOFs building blocks into required structures or platforms for designing new kinds of hierarchical morphologies, which to our knowledge has not been previously investigated.

Keywords: ZIF-8; composite materials; polymerization of alkylsilane; siloxane microflowers; fabrication of MOF

1. Introduction

Recently, metal-organic frameworks (MOFs), a type of functional porous organometallic compound material, have aroused widespread attention due to their powerful attributes of structural and chemical versatility and tailorability [1]. These kinds of materials also have well-organized networks composed of metal cations and organic electron donor linkers [2]. These properties make MOFs ideal candidates for many fields [3–10]. A number of heterogeneous catalytic reactions such as hydrogenation, oxidation, photocatalysis, carbonyl cyanosilylation, and hydrodesulfurization [11] have been driven by MOFs successfully. However, there are extremely rare works on MOFs as polymerization catalysts. For example, a series of Zn-based MOFs (zinc carboxylates) have been shown capable of polymerizing propylene oxide with CO_2 or any substance delivering CO_2 to produce polycarbonates [12]. A titanium-organic framework, which is an air-stable material, acted as a high-activity trigger for the ring-opening polymerization of cyclic esters [13]. Futhermore, Nd-based MOFs have been shown to be pre-catalysts for the polymerization of isoprene, when combined with aluminoxanes [14]. Thus, current studies on these aspects are mainly concentrated on unsaturated

hydrocarbon molecules. Additionally, the polymerization reaction is rarely reported using saturated alkanes as the reactants. Studies about the effect of catalysts on the morphologies of polymerization products are also very limited.

Meanwhile, siloxane polymers are an important class of chemical products widely used in fire resistance [15], pharmacy fields [16], and thermal protection systems [17]. There have been a few reports on the preparation of siloxanes with hybrid nano- and micro-structures by the aggregation of saturated alkylsilanes ($C_{18}H_{37}SiH_3$, ODS), originally using noble metal nanoparticles as catalysts [18–22]. Ternary chalcogenide compounds ($AgBiS_2$) and polyvinyl pyrrolidone-capped silver nanoparticles have also been confirmed to be able to catalyze the polymerization of alkylsilanes to form polysiloxanes [19–21] in our previous works. In addition, a noble metal salt, as a homogeneous catalyst, was also used to synthesize siloxane nanowires and hybrid metal core-siloxane shell nanoparticles [22]. However, there is little discussion about these routes for controlling the topography and shape of the final products. Indeed, no work has been reported for directly using MOFs as a catalyst for polymerizing alkylsilanes thus far.

Recently, there have been some reports on utilizing MOFs as sacrificial templates to prepare different nanomaterials such as Fe_2O_3/TiO_2 photocatalysts [23], ZnO@C composites [24], hollow silica rods [25], and hollow ZnS polyhedrals [26], because of the diverse morphologies of MOFs. Interestingly, nanoporous carbon, considered as a material with vital hydrogen storage capacity and unexpected high surface area, has been synthesized utilizing a zeolitic imidazolate framework-8 (ZIF-8) as both a template and precursor [27]. Although some progress has been made, research on the gentle preparation of functional MOFs materials with hierarchical and complex morphologies is still in its preliminary stages and remains a significant challenge [28]. Therefore, it is highly desirable to find facile novel synthetic concepts and protocols using MOFs to synthesize functional materials with special morphologies in the absence of unsaturated hydrocarbon molecules.

In this work, we explored the role of ZIF-8 during the polymerization process of alkylsilanes ($C_{18}H_{37}SiH_3$, ODS) without an initiator and/or cocatalyst. ZIF-8 was used because of its good thermal, hydrothermal, and chemical stabilities. The six-membered-ring pore windows of ZIF-8 are 3.4 Å, which are narrow enough to inhibit the accessibility of bulky molecules such as alkylsilan ($C_{18}H_{37}SiH_3$, ODS) into the pore cavities [29]. Meanwhile, the polymerization reaction can be finished on the surface of ZIF-8. It will be worthwhile to explore the unexpected polymerization of large molecules. Under room temperature conditions, the polymerization reaction occurring by the use of homogeneous noble metal salt as a catalyst has been reported [22]. Furthermore, we successfully make this reaction occur under the same conditions by using ZIF-8. As a result, hybrid ZIF-8/siloxane microspheres and rose petal-like composites were fabricated.

2. Results and Discussion

In this research, ZIF-8 was obtained by the direct reaction of zinc hydroxide to 2-methylimidazole at ambient temperature [30]. The scanning electron microscopy (SEM) image (Figure S1a) shows that micrometer-sized crystals have the uniform cubic shapes of ZIF-8. Transmission electron microscopy (TEM) (Figure S1b) revealed that ZIF-8 particles were nanocrystals with sharp hexagonal facets, with the size distribution of ZIF-8 in the range of 100–200 nm. As shown in Figure S1, the size and morphology of ZIF-8 are the same as that reported previously [31]. Figure S2 shows the X-ray diffraction (XRD) patterns of ZIF-8 with the scanning range from 0° to 40°. The strong diffraction peaks appearing at 7.26°, 10.3°, 12.64°, 17.94°, and 26.56° are consistent with the XRD patterns of ZIF-8 [31] and show that ZIF-8 nanoparticles were successfully synthesized. Meanwhile, the prepared ZIF-8 is a pure phase and does not contain impurity peaks. The N_2 adsorption-desorption isotherm is shown in Figure S3, indicating a type I isotherm. The Brunner−Emmet−Teller (BET) surface area is 1404.2 m^2/g [32] and the pore volume and average pore size are 0.68 $cm^3 \cdot g^{-1}$ and ca. 12 nm, respectively, which are comparable to that reported by Kyo et al. [33].

The polymerization experiments were conducted with some modifications to the procedure reported by Prasad et al. [18]. The reactions were firstly carried out at 90 °C as in our previous studies [19–21]. A significant change in intensity at the wavenumber of 2150 cm^{-1} was observed in the FT-IR spectra owing to the stretching peak of Si-H (Figure 1c), using 10 mg ZIF-8 for 4 h. The Si-H bonds' absorption of the obtained product became weaker than that of pure $C_{18}H_{37}SiH_3$. Meanwhile, a new stretching vibration absorption at 1110 cm^{-1} appeared, indicating that the polymerization of octadecylsilane occurred (Figure 1a,c) [19]. This was not observed in unconverted octadecylsilane. At 2854 cm^{-1} and 2925 cm^{-1}, the absorption peaks are associated with the symmetric and asymmetric stretching vibrations of CH_2 in the alkyl chains. Moreover, two bands at 2933 cm^{-1} and 3138 cm^{-1} were also observed in the spectra of the ZIF-8 due to the C-H stretching vibration bonds in the imidazole ring and the methyl group, respectively. The control experiments were conducted without ZIF-8. The FT-IR spectra confirmed that the octadecylsilane was not polymerized because the band at 1110 cm^{-1} which corresponds to Si-O stretching vibration did not appear in the absence of ZIF-8. Interestingly, the polymerization of octadecylsilane over ZIF-8 could even occur at a lower temperature close to ambient conditions (about 20 °C to 30 °C), even though the product obtained at 30 °C has a weaker Si-O characteristic band in the FT-IR spectra in comparison with the product obtained at 90 °C (Figure 1b). It has been reported before that by only using homogeneous noble metal salt as a catalyst, this polymerization reaction could take place at room temperature [22]. Furthermore, as shown in Figure 1, the FT-IR spectra of the polymerization product using 10 mg ZIF-8 also showed the characteristic absorptions of ZIF-8. The band at 1590 cm^{-1} is assigned to the stretching vibration of C=N. The peaks at 1350–1500 cm^{-1} corresponded to the entire imidazole ring stretching. The bands in the spectral region of 900–1350 cm^{-1} are associated with the in-plane bending of the imidazole ring and the bands below 800 cm^{-1} correspond to the out-of-plane bending [34]. The XRD pattern of recovered ZIF-8 after removal of the polymerized products by o-xylene also corresponded with the pure ZIF-8 (Figure S4). These observations confirmed that the MOFs maintained their structures during the reaction. Therefore, it is clearly suggested that ZIF-8 played the role of catalyst in the polymerization reaction.

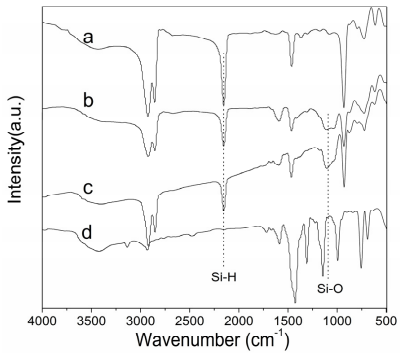

Figure 1. Fourier transform infrared spectra (FT-IR) spectra of (**a**) pure $C_{18}H_{37}SiH_3$ products of polymerization of $C_{18}H_{37}SiH_3$ catalyzed by using 0.01 g ZIF-8; (**b**) at 30 °C; (**c**) at 90 °C; (**d**) pure ZIF-8.

The SEM images revealed that siloxane polymers obtained below 30 °C were microspheres (Figure 2a and Figure S5a,b) with diameters of 5–7 μm. Each microsphere exhibited a bird's nest morphology, which was formed from numerous nanosheets (50 to 80 nm in thickness). The nanosheets exhibited a rough appearance, grew in all directions, and were curled and interlaced tightly. When the reaction temperature was increased to 60 °C, several dozens of intercrossed nanosheets (60 to 180 nm in thickness) were not highly concentrated and bloomed into rose petal-like structures (Figure 2b). These rose petal-like products maintained their integrity even when the temperature was increased to 90 °C and 120 °C (Figure 2c–d). Interestingly, the polymerization reaction could occur in 5 min at 90 °C, and poorly-formed flowery structures constructed by many nanosheets were obtained

(Figure 3a). Prolonging the reaction time to 1 h produced rose-petal microflowers as the dominant products (Figure 3b), and only a few solid spheres remained. For a reaction time of 2–12 h, well-defined microflowers were formed, which consisted of nanosheets (40 to 180 nm in thickness, Figure 3c–f). In order to explore the growth process, we also carried out the control experiment at 30 °C. When the reaction was terminated after 5 min at 30 °C, neither microspheres nor rose petal-like microflowers were observed, except for ZIF-8 nanocrystals (Figure S5c), indicating that the octadecylsilane was not polymerized during the 5 min. When the reaction time was extended to 12 h, the bird's nest morphology which could be obtained in 4 h disappeared. Only some layered structures and ZIF-8 nanocrystals remained (Figure S5d), indicating that the microsphere structures were not stable at longer reaction times. This phenomenon revealed that the structure of the products obtained at 30 °C was unstable when compared with the products obtained at 90 °C. A stable structure is prone to form at a higher temperature. The amount of catalyst had little effect on the morphologies of the final products (Figure S6).

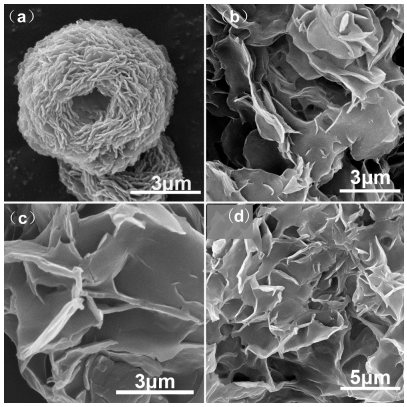

Figure 2. Scanning electron microscopy (SEM) images of the polymerization products of $C_{18}H_{37}SiH_3$ by 0.01 g ZIF-8 for 4 h at (**a**) 30 °C; (**b**) 60 °C; (**c**) 90 °C; (**d**) 120 °C.

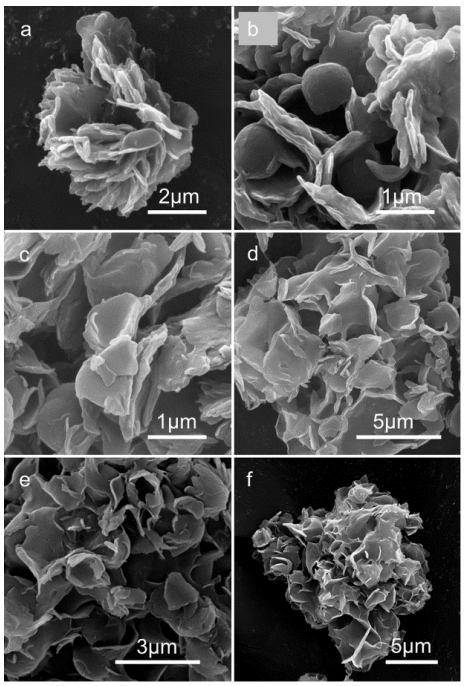

Figure 3. SEM images of the polymerization products of $C_{18}H_{37}SiH_3$ by 0.01 g ZIF-8 at 90 °C (**a**) 5 min; (**b**) 1 h; (**c**) 2 h; (**d**) 4 h; (**e**) 6 h; (**f**) 12 h.

The as-obtained polymerization products at 30 °C and 90 °C were further characterized by TEM. As shown in Figure S7a, the sheets of the products obtained at 30 °C had spherical structures. Figure S7b shows the sheet structures of the rose petal-like products obtained at higher temperature. The SEM images (Figure 2) are in accordance with these results. Figure S7 also revealed the presence of ZIF-8 in the interior of each microstructure. This further confirmed that the ZIF-8 acted as a nucleation center for polymerizing silane, and the polymerization reaction was carried out on the surface of ZIF-8, which was in accordance with the XRD results (Figure S4).

The surface information of the polymerization products was analyzed by X-ray photoelectron spectra measurement (XPS). As shown in Figure 4, the red full lines are experimental curves and the black lines are calculated curves. The narrow scan spectra of Si 2p (Figure 4) shows that the binding energy values of Si 2p are 101.0 eV and 102.0 eV, which could be attributed to Si–H [21] and Si–O [21] bonds, respectively. The formation of the Si–O bond could be promoted by increasing the amount of ZIF-8 or by raising the reaction temperature. Accordingly, the contribution of Si–O in the products increased from 8.8% (Figure 4a) to 39.7% (Figure 4c), and the intensity of Si–H bond declined from 91.2% (Figure 4a) to 60.3% (Figure 4c), indicating the degree of the polymerization reaction increased at higher temperature. This was in agreement with the Fourier transform infrared spectra (FT-IR) results.

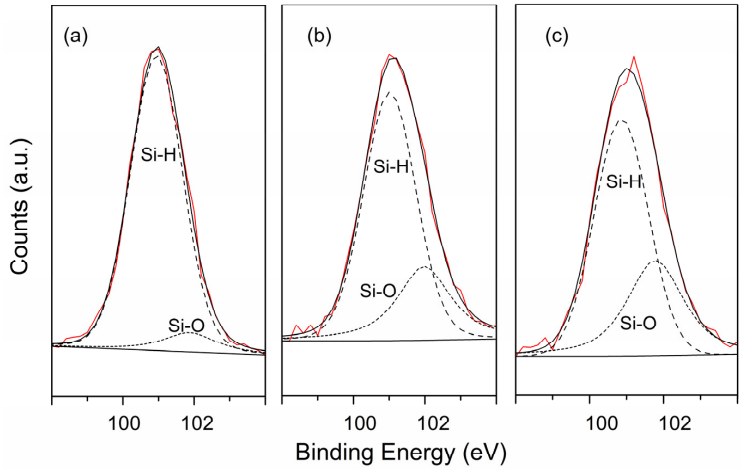

Figure 4. X-ray photoelectron spectra (XPS) spectra of the polymerization products of $C_{18}H_{37}SiH_3$ by using (**a**) 0.01 g ZIF-8 30 °C; (**b**) 0.01 g ZIF-8 90 °C; (**c**) 0.03 g ZIF-8 90 °C.

Although the exact mechanism for the formation of hierarchical siloxane structures is not clear, based on the literature [18–22] and the results in the current study, we propose that the monomer molecule of ODS assembled and polymerized, and finally formed the novel hierarchical structures. The ZIF-8 nanocrystals catalyzed the polymerization reaction and oriented the growth of the siloxane polymers. The small pore windows of ZIF-8 (3.4 Å) [35] might inhibit the accessibility of bulky molecules entering into the pore cavities [29]. Therefore, the polymerization of alkylsilanes should be initiated on the external surface of MOFs. A possible growth process has been proposed as follows: At the beginning of the reaction, the octadecylsilane molecules attached to the surface active site (Zn^{2+}) [30] of the polyhedral ZIF-8 to form weak Zn–Si bonds. Water molecules might easily attack these weak bonds, resulting in the formation of $Si(OH)_x$ [18]. The $RSi(OH)_x$ molecules then reacted with each other, building Si–O–Si bonds and growing into hierarchical structures under the direction of the ZIF-8 nanocrystals or in the liquid phase. Microslice structures that were first formed self-assembled into the microspheres below 30 °C. When the reaction temperature increased, the microslices self-assembled into rose petal-like microstructures, indicating that the microspherical structures were kinetically controlled and the flower microstructure products were thermodynamically controlled. The morphologies of the products polymerized by using ZIF-8 were more uniform in comparison with those catalyzed by the noble metal nanoparticles and ternary chalcogenide

semiconducting compounds. To determine whether the dissolved homogeneous or heterogeneous Zn^{2+} species were the catalysts responsible for the polymerization reaction, a polymerization reaction using $Zn(NO_3)_2$ was carried out. Only layer structures were observed by SEM (Figure S8), indicating that the framework of ZIF-8 played a vital role in the process.

Moreover, the melting points of the products obtained by using 10 mg ZIF-8 at 30 °C and 90 °C for 4 h were measured to be 48 °C and 52 °C, respectively. Obviously, the melting points of the products were significantly higher when compared with octadecylsilane (29 °C). Furthermore, the ZIF-8-polymer composite products with hierarchical structures had a water contact angle of 107.9° (Figure S9b) which is higher than that of ZIF-8 (82.5°, Figure S9a). The polymerization composites could have potential applications in thermal resistance [15], surface self-cleaning, waterproofing, or antifouling fields [36].

3. Materials and Methods

3.1. Synthesis of ZIF-8

ZIF-8 was prepared with 2-methylimidazole and zinc hydroxide according to the literature [30]. In a typical synthesis, zinc hydroxide (3.904 g) was dissolved in aqueous ammonia (25% v/v, 500 mL). Then a solution containing 2-methylimidazole (6.442 g) in methanol (100 mL) was slowly added under stirring. White polyhedral crystals formed immediately and the reaction mixture was stirred softly for two days. After this, the white crystals were separated by filtration and thoroughly washed several times with a H_2O/MeOH (1:1 v/v) mixture. Then the products were dried under vacuum in an oven at 90 °C.

3.2. Polymerization of Octadecylsilane over ZIF-8

The route for polymerizing octadecylsilane catalyzed by gold nanoparticles was similar to that described by references [18–21]. The polymerizations of octadecylsilane in this work were carried out in a round-bottom flask under magnetic stirring. Unless otherwise stated, the mixture of ZIF-8 (0.01 g) and octadecylsilane (0.2 g) was put in a 25 mL flask with butanone (10 mL) and a small amount of water (10 μL). After the reaction, the mixture was centrifuged and the acquired solid was dried at room temperature.

3.3. Characterizations

Fourier transform infrared (FT-IR) spectra were obtained on a Thermo Nicolet 8700 instrument (Thermo Fisher Scientific, Waltham, MA, USA), with 1% of the samples being dispersed on potassium bromide pallets. Sixty-four scans were taken for each spectrum in transmission at a spectral resolution of 4 cm^{-1}. Scanning electron microscopy (SEM) was performed using a Philips XL-30ESEM-TMP microscope (FEI, Hillsboro, OR, USA). Transmission electron microscopy (TEM) was conducted on a Hitachi H-800 instrument (Japan Electron Optics Laboratory CO., LTD, Tokyo, Japan) at an accelerating voltage of 150 kV. X-ray diffraction (XRD) patterns were recorded on a Rigaku TTRIII diffractometer (Rigaku Co., Tokyo, Japan) with Cu Kα radiation in the 2θ range of 3°–90° at a scan rate of 10°/min. The nitrogen adsorption/desorption isotherms were measured by using automatic volumetric adsorption equipment (Micromeritics Instrument Corp., Norcross, GA, USA). The X-ray photoelectron spectra (XPS) measurement was performed on a PHI5000 Versa Probe II analyzer (Shimadzu Corp., Kyoto, Japan).

4. Conclusions

In summary, for the first time, ZIF-8 was shown to be able to induce the polymerization of alkylsilanes to fabricate 3D microspheres and rose petal-like products at different reaction temperatures. The obtained products are more thermally stable than octadecylsilane and are hydrophobic. This work not only extends the applicability of MOFs, but also develops a rational unique way to utilize MOFs

for the multidimensional assembly of MOFs building blocks into required structures or platforms in catalytic polymerization.

Supplementary Materials: The following are available online at www.mdpi.com/2073-4344/7/3/77/s1, Figure S1: (a) SEM image of pure ZIF-8 particles; (b) TEM image of pure ZIF-8 particles, Figure S2: Powder XRD pattern for ZIF-8 nanoparticles before the reaction, Figure S3: Nitrogen sorption isotherms of as-synthesized ZIF-8 nanocrystals at 77 K. Black and red data correspond to the adsorption and desorption branches, respectively, Figure S4: XRD patterns of pure ZIF-8 (a), ZIF-8 treated by *o*-xylene before the polymerization reaction (b), ZIF-8 treated by o-xylene after the polymerization reaction (c), Figure S5: SEM images of the polymerization products of $C_{18}H_{37}SiH_3$ by 0.01 g ZIF-8 at (a) 20 °C, 4 h; (b) 30 °C, 4 h; (c) 30 °C, 5 min; (d) 30 °C, 12 h, Figure S6: SEM images of the polymerization products of $C_{18}H_{37}SiH_3$ at 90 °C for 4 h (a) 0.01 g ZIF-8; (b) 0.02 g ZIF-8; (c) 0.03 g ZIF-8, Figure S7: TEM images of the polymerization products of $C_{18}H_{37}SiH_3$ by ZIF-8 at (a) 30 °C, (b) 90 °C, Figure S8: SEM images of the reaction products by using $Zn(NO_3)_2$ at 30 °C for 4 h (a,b); at 90 °C for 4 h (c,d), Figure S9: The profiles of water droplets on (a) ZIF-8, (b) and the polymerization products of $C_{18}H_{37}SiH_3$ by ZIF-8.

Acknowledgments: This work was supported by the National Natural Science Foundation of China (21263027, 21573193, 21367024 and 21403190) and Yunnan Applied Basic Research Projects (2016FA002, 2016FD009). The authors also thank the Program for Innovation Team of Yunnan Province, Key Laboratory of Advanced Materials for Waste Water Treatment of Kunming and the Key project from the Yunnan Provincial Education Department of Science Research Fund (Project 2016CYH04), and the Program for Science and Technology Projects of Yunnan Industrial of China Tobacco Industry CO. of Yunnan Province, Ltd. (2016539200340108) for financial support.

Author Contributions: W.W. and J.W. conceived and designed the experiments; J.Z., L.Y., and C.X. performed the experiments; Y.L. and L.G. analyzed the data; Y.C., L.Y., and C.X. wrote the paper; L.Y., C.X., M.N. and Z.Y. modified the paper.

Conflicts of Interest: The authors declare no conflict of interest.

References

1. Falcaro, P.; Buso, D.; Hill, A.J.; Doherty, C.M. Patterning techniques for metal organic frameworks. *Adv. Mater.* **2012**, *24*, 3153–3168. [CrossRef] [PubMed]
2. Meek, S.T.; Greathouse, J.A.; Allendorf, M.D. Metal-organic frameworks: A rapidly growing class of versatile nanoporous materials. *Adv. Mater.* **2011**, *23*, 249–267. [CrossRef] [PubMed]
3. Abid, H.R.; Pham, G.H.; Ang, H.M.; Tade, M.O.; Wang, S. Adsorption of CH_4 and CO_2 on Zr-metal organic frameworks. *J. Colloid Interf. Sci.* **2012**, *366*, 120–124. [CrossRef] [PubMed]
4. Roberts, J.M.; Fini, B.M.; Sarjeant, A.A.; Farha, O.K.; Hupp, J.T.; Scheidt, K.A. Urea metal-organic frameworks as effective and size-selective hydrogen-bond catalysts. *J. Am. Chem. Soc.* **2012**, *134*, 3334–3337. [CrossRef] [PubMed]
5. Farrusseng, D.; Aguado, S.; Pinel, C. Metal-organic frameworks: opportunities for catalysis. *Angew. Chem. Int. Ed. Engl.* **2009**, *48*, 7502–7513. [CrossRef] [PubMed]
6. Ranocchiari, M.; Bokhoven, J.A. Catalysis by metal-organic frameworks: fundamentals and opportunities. *Phys. Chem. Chem. Phys.* **2011**, *13*, 6388–6396. [CrossRef] [PubMed]
7. Maksimchuk, N.V.; Kovalenko, K.A.; Fedin, V.P.; Kholdeeva, O.A. Heterogeneous Selective Oxidation of Alkenes to α,β-Unsaturated Ketones over Coordination Polymer MIL-101. *Adv. Synth. Catal.* **2010**, *352*, 2943–2948. [CrossRef]
8. Dhakshinamoorthy, A.; Alvaro, M.; Garcia, H. Commercial metal-organic frameworks as heterogeneous catalysts. *Chem. Commun.* **2012**, *48*, 11275–11288. [CrossRef] [PubMed]
9. Ameloot, R.; Roeffaers, M.B.; Cremer, D.G.; Vermoortele, F.; Hofkens, J.; Sels, B.F.; Vos, D.E. Metal-organic framework single crystals as photoactive matrices for the generation of metallic microstructures. *Adv. Mater.* **2011**, *23*, 1788–1791. [CrossRef] [PubMed]
10. Zhou, M.; Wu, Y.N.; Qiao, J.; Zhang, J.; McDonald, A.; Li, G.; Li, F. The removal of bisphenol A from aqueous solutions by MIL-53(Al) and mesostructured MIL-53(Al). *J. Colloid Interf. Sci.* **2013**, *405*, 157–163. [CrossRef] [PubMed]
11. Corma, A.; García, H.; Xamena, F.X. Engineering Metal Organic Frameworks for Heterogeneous Catalysis. *Chem. Rev.* **2010**, *110*, 4606–4655. [CrossRef] [PubMed]
12. Mller, U.; Luinstra, G.; Yaghi, O.M. Process for Producing Polyalkylene Carbonates. US Patent 6,617,467 B1, 9 September 2003.

13. Christopher, J.C.; Matthew, G.D.; Matthew, D.J.; Gabriele, K.K.; Matthew, D.L.; Stephen, W. Air-Stable Titanium Alkoxide Based Metal-Organic Framework as an Initiator for Ring-Opening Polymerization of Cyclic Esters. *Inorg. Chem.* **2006**, *45*, 6595–6597.
14. Vitorino, M.J.; Devic, T.; Tromp, M.; Férey, G.; Visseaux, M. Lanthanide Metal-Organic Frameworks as Ziegler-Natta Catalysts for the Selective Polymerization of Isoprene. Macromol. *Chem. Phys.* **2009**, *210*, 1923–1932.
15. Antonietta, G.; Robert, S.A. Fire performance of poly(dimethyl siloxane) composites evaluated by cone calorimetry. *Compos. Part A-Appl. Sci. Manuf.* **2008**, *39*, 398–405.
16. Farhang, A.; Hamid, M.; Ali-Asgar, K. Modification of polysiloxane polymers for biomedical applications: A review. *Polym. Int.* **2001**, *50*, 1279–1287.
17. Yang, D.; Zhang, W.; Jiang, B.; Guo, Y. Silicone rubber ablative composites improved with zirconium carbide or zirconia. *Compos. Part A Appl. Sci. Manuf.* **2013**, *44*, 70–77. [CrossRef]
18. Prasad, B.L.V.; Savka, I.S.; Christopher, M.S.; Vladimir, Z.; Kenneth, J.K. Gold Nanoparticles as Catalysts for Polymerization of Alkylsilanes to Siloxane Nanowires, Filaments, and Tubes. *J. Am. Chem. Soc.* **2003**, *125*, 10488–10489. [CrossRef] [PubMed]
19. Yan, J.; Zi, G.; Yang, F.; Mi, Y.; Yang, X.; Wang, W.; Zou, Q.; Wang, J. The polymerizations of alkylsilane and bis-(γ-triethoxysilylpropyl)-tetrasulfide catalyzed by copper nanoparticles and the effects of transition metal ions on the polymerizations of alkylsilane catalyzed by silver nanoparticles. *Mater. Chem. Phys.* **2009**, *118*, 513–518. [CrossRef]
20. Wei, Q.; Li, B.; Li, C.; Wang, J.; Wang, W.; Yang, X. PVP-capped silver nanoparticles as catalysts for polymerization of alkylsilanes to siloxane composite microspheres. *J. Mater. Chem.* **2006**, *16*, 3606. [CrossRef]
21. Wang, J.; Yang, X.; Hu, W.; Li, B.; Yan, J.; Hu, J. Synthesis of $AgBiS_2$ microspheres by a templating method and their catalytic polymerization of alkylsilanes. *Chem. Commun.* **2007**, 4931–4933. [CrossRef]
22. Goyal, A.; Kumar, A.; Ajayan, P.M. Metal salt induced synthesis of hybrid metal core-siloxane shell nanoparticles and siloxane nanowires. *Chem. Commun.* **2010**, *46*, 964–966. [CrossRef] [PubMed]
23. De Krafft, K.E.; Wang, C.; Lin, W. Metal-organic framework templated synthesis of Fe_2O_3/TiO_2 nanocomposite for hydrogen production. *Adv. Mater.* **2012**, *24*, 2014–2018. [CrossRef] [PubMed]
24. Yang, S.J.; Im, J.H.; Kim, T.; Lee, K.; Park, C.R. MOF-derived ZnO and ZnO@C composites with high photocatalytic activity and adsorption capacity. *J. Hazard. Mater.* **2011**, *186*, 376–382. [CrossRef] [PubMed]
25. William, J.R.; Kathryn, L.T.; Lin, W. Surface Modification and Functionalization of Nanoscale Metal-Organic Frameworks for Controlled Release and Luminescence Sensing. *J. Am. Chem. Soc.* **2007**, *129*, 9852–9853.
26. Jiang, Z.; Sun, H.; Qin, Z.; Jiao, X.; Chen, D. Synthesis of novel ZnS nanocages utilizing ZIF-8 polyhedral template. *Chem. Commun.* **2012**, *48*, 3620–3622. [CrossRef] [PubMed]
27. Jiang, H.L.; Liu, B.; Lan, Y.Q.; Kuratani, K.; Akita, T.; Shioyama, H.; Zong, F.; Xu, Q. From metal-organic framework to nanoporous carbon: toward a very high surface area and hydrogen uptake. *J. Am. Chem. Soc.* **2011**, *133*, 11854–11857. [CrossRef] [PubMed]
28. Zhang, L.; Wu, H.B.; Madhavi, S.; Hng, H.H.; Lou, X.W. Formation of Fe_2O_3 microboxes with hierarchical shell structures from metal-organic frameworks and their lithium storage properties. *J. Am. Chem. Soc.* **2012**, *134*, 17388–17391. [CrossRef] [PubMed]
29. Uyen, N.T.; Ky, A.L.; Nam, S.P. Expanding Applications of Metal—Organic Frameworks: Zeolite Imidazolate Framework ZIF-8 as an Efficient Heterogeneous Catalyst for the Knoevenagel Reaction. *ACS Catal.* **2011**, *1*, 120–127.
30. Céline, C.; Sandrine, L.; Delphine, B.; Fabien, B.; Vincent, L.; Emmanuel, S.; Anne-Agathe, Q.; Nicolas, B. Catalysis of Transesterification by a Nonfunctionalized Metal-Organic Framework: Acido-Basicity at the External Surface of ZIF-8 Probed by FTIR and ab Initio Calculations. *J. Am. Chem. Soc.* **2010**, *132*, 12365–12377.
31. Yichang, P.; Yunyang, L.; Gaofeng, Z.; Lan, Z. Rapid synthesis of zeolitic imidazolate framework-8 (ZIF-8) nanocrystals in an aqueous system. *Chem. Commun.* **2011**, *47*, 2071–2073.
32. Kai, X.; Shuai, C.; Xiaoyu, P.; Caterina, D. Carbon with hierarchical pores from carbonized metal—Organic frameworks for lithium sulphur batteries. *Chem. Commun.* **2013**, *49*, 2192–2194.
33. Kyo, S.P.; Zheng, N.; Adrien, P.C.; Jae, Y.C. Exceptional chemical and thermal stability of zeolitic imidazolate frameworks. *Proc. Natl. Acad. Sci. USA* **2006**, *103*, 10186–10191.
34. Hu, Y.; Kazemian, H.; Rohani, S.; Huang, Y.; Song, Y. In situ high pressure study of ZIF-8 by FTIR spectroscopy. *Chem. Commun.* **2011**, *47*, 12694–12696. [CrossRef] [PubMed]

35. Na, C.; Zhi, Y.G.; Xiu, P.Y. Zeolitic Imidazolate Framework-8 Nanocrystal Coated Capillary for Molecular Sieving of Branched Alkanes from Linear Alkanes along with High-Resolution Chromatographic Separation of Linear Alkanes. *J. Am. Chem. Soc.* **2010**, *132*, 13645–13647.
36. Jiang, L.; Zhao, Y.; Zhai, J. A lotus-leaf-like superhydrophobic surface: A porous microsphere/nanofiber composite film prepared by electrohydrodynamics. *Angew. Chem. Int. Ed. Engl.* **2004**, *43*, 4338–4341. [CrossRef] [PubMed]

© 2017 by the authors. Licensee MDPI, Basel, Switzerland. This article is an open access article distributed under the terms and conditions of the Creative Commons Attribution (CC BY) license (http://creativecommons.org/licenses/by/4.0/).